MONITORING CATHODIC SHIELDING AND CORROSION UNDER DISBONDED COATINGS

F. Varela, M. YJ Tan, B. Hinton, M. Forsyth
Institute for Frontier Materials, Deakin University, Victoria 3220, Australia

ABSTRACT: This work presents a novel corrosion monitoring probe designed for simulating the conditions developed under disbonded coatings and for measuring current densities and their distribution over a simulated pipeline surface. The probe's concept was experimentally evaluated via immersion tests under Cathodic Protection (CP) in high resistivity aqueous solution. Under the disbonded area, anodic currents as well as cathodic currents were both measured. Anodic current densities were used to calculate metal losses by means of Faraday's law. Calculated corrosion patterns were compared with corrosion damage observed at the probe's surface after a period of test. The probe's working principles are explained in terms of simple electrochemistry.

Keywords: Pipeline, Steel, Disbonded coating, Cathodic protection, Corrosion monitoring.

1. INTRODUCTION

Corrosion monitoring is often based on the simulation of environmental conditions on a large and complex structure such as a buried pipeline using a small probe, and the measurement of the thermodynamics and kinetics of corrosion processes occurring on the probe surface. If corrosion processes are properly simulated, the probe can provide useful information on corrosion over the larger structure. This concept has been successfully implemented in many industries such as the petrochemical industry, however, corrosion monitoring of underground pipelines remains a challenge. The highly resistive soil environment, the use of impressed current cathodic protection (CP) systems and the presence of barrier coatings make corrosion monitoring difficult. For instance CP introduces a great complication to traditional electrochemical corrosion monitoring techniques because they are only applicable around the open circuit potential [1-3]. The application of non-electrochemical techniques such as corrosion coupons can also be difficult for underground applications because of the need for costly underground installation/extractions. Corrosion coupons would only be able to provide time averaged information after a long exposure to the environment. Electrical resistance probes can provide in-situ data, however in principle they are unable to measure localised corrosion because localised damages such as pitting may not lead to any significant change in electric resistance. Unfortunately localised forms of corrosion are often the type of attack found in pipelines.

On the other hand, the use of barrier coatings on pipelines introduces some other complexities for corrosion monitoring. For instance a common form of pipeline damage is related to coating disbondment that generates a crevice between the disbonded coating film and the metallic pipe. This type of coating defect requires particular attention since it is found to be related to the most severe localised corrosion issues in pipelines [4-7]. It is known from published modelling and experimental works that the environment under disbonded coatings deviates significantly from the bulk. Due to the shielding of CP currents and isolation of the external environment, the crevice area develops a complex environment with high cation concentrations [8-11], high pH (in most cases) [8-10, 12-17], negligible oxygen [9, 10, 12, 15-18] and a gradient of potentials [8, 9, 11-22]. The initiation and propagation of localised corrosion under disbonded pipeline coatings are considered to be extremely challenging to monitor; at present there is no sensor technology that possesses the abilities of providing in-situ information regarding them [19].

The purpose of this paper is to develop a new CP compatible localised corrosion monitoring method for the pipeline industry. The most important component of the method is a novel corrosion monitoring probe that is capable of simulating the evolution of the environment under disbonded coatings and measure the initiation and propagation of localised corrosion under disbonded pipeline coatings under CP.

2. METHOD AND EXPERIMENTAL PROCEDURE

As shown in Figure 1, a novel corrosion monitoring probe was designed for simulating and evaluating current density profiles along a simulated coating disbondment area. The probe's design is based on an interconnected electrode array.

Closely packed electrode arrays allow the simulation of a metallic surface while independent electrochemical measurements between wires can be performed [23, 24]. This design allows proper simulation of the gradients of pH, nonuniform oxygen distribution and lack of CP effectiveness by exposing the array to inhomogeneous conditions under a simulated disbonded coating layer.

2.1 Experimental Setup

For the proof of concept, a probe was made based on a Wire Beam Electrode (WBE) consisting of a one hundred 1.59mm diameter UNS no. G0350 wires mounted in epoxy in a 10 by 10 array of 18.5 by 18.5mm. Figure 1 presents a schematic view of this electrode array and the rest of the probe assembly. To simulate a perfectly CP shielding disbonded coating, a polymethyl methacrylate (PMMA) cover was used. The cover did not shield the whole array; instead the first two rows of electrodes were left to simulate a coating defect. A rubber seal was used to prevent the solution ingress around the edges of the electrode array. This seal was held in place by a groove machined in the PMMA cover. The array surface was abraded to 1200 grit using silicon carbide paper and using water as lubricant. After abrading, the array was immediately rinsed with ethanol and acetone. The simulated disbonded coating was then installed on top of the array using four stainless steel 316 screws. To achieve an even crevice gap of 0.25mm, cellophane film fragments were used

Figure 1. New probe's assembly

as spacers by placing them in the locations indicated in figure 1. A schematic representation of the experimental setup used is presented in figure 2. The probe was installed in a 2.5L electrochemical cell.
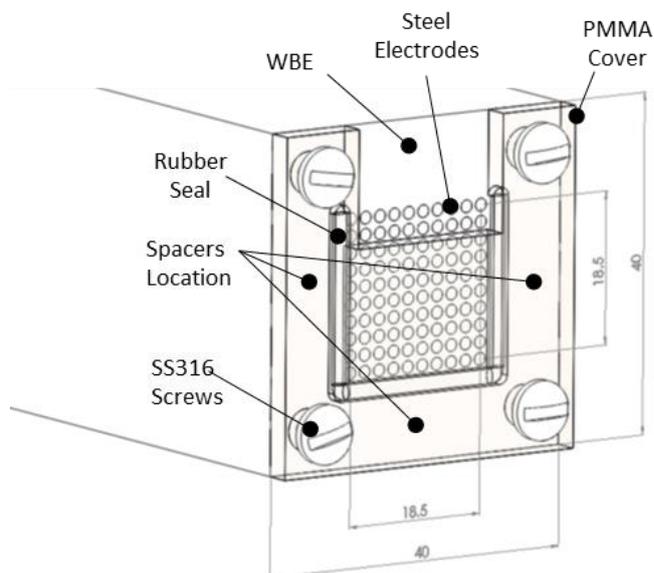
The probe was connected to a programmable multiplexer and measuring instrument using computer cables. To measure the net current values at each electrode, a Zero Resistance Ammeter (ZRA) was interconnected between WE1 and WE2. At any time 99 electrodes were connected to WE1 and the remaining electrode was connected to the WE2 (see Figure 2). All

Figure 2. Experimental set up

potentials were measured against a Ag/AgCl/Sat. KCl reference electrode (Ref.). The ZRA allowed to achieve the same electrical potential between WE1 and WE2, maintaining all electrodes constantly under CP. CP was applied by fixing the probe's potential at $-760mV_{Ag/AgCl}$ ($-850mV_{CSE}$), using a potentiostat in a traditional three electrodes configuration where WE1 was used as working electrode (WE). Counter Electrodes (CE) consisted of two Ø4.5mm graphite rods of 120mm long were immersed in the test solution to provide CP to the system. To minimize IR drops, a Luggin capillary was used.
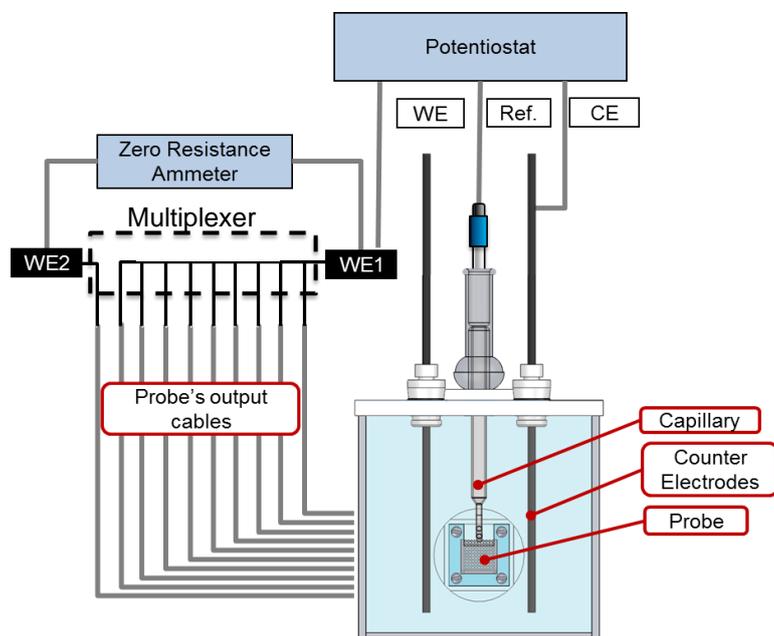
A test solution representative of highly resistive soils was used in this test. The 5000 ohm.cm, 0.001M Na_2SO_4 test solution was prepared from analytical grade reagents and ASTM D1193 ultrapure water [25]. Air was purged through the solution for at least 2h before the test to ensure an initial oxygen saturation concentration. The test was performed in an open to air condition. During the test, current scans were performed every 20min for the 23h immersion period. Tests were

performed in duplicates at room temperature (22°C).

A post processing script for MATLAB was used to analyse the local current data recorded by the ZRA. This script constructed current density distribution maps based on the ZRA data, the multiplexer scanning sequence and the electrodes addresses. Current densities were calculated based on the area of a single electrode (1.98mm^2). An Evan's diagram, as shown in Figure 3, was used to aid the interpretation of the current distribution maps. A metal losses map was also calculated by applying Faraday's law to the accumulated charge of the anodic currents registered by the probe.

3. RESULTS AND DISSCUSION

Figure 4 presents the current density distribution maps obtained by the probe at different immersion times over a 22 hour test period. Anodic current densities are represented by positive values while cathodics are represented by negatives values. The first two rows of each current density map corresponds to the uncovered electrodes area (simulating coating defect areas), while the rest show the behaviour within the area under the crevice (simulating disbonded coating areas).

In general, large cathodic current densities were found at the uncovered electrode areas. Anodic current densities were only detected under the disbonded area and the value decreased as the test progressed. The CP current profiles obtained with the probe (see Figure 4) correlate well with the results presented in other published works where significantly larger cathodic current densities were reported at the crevice opening [11, 18, 20, 26, 27]. However, anodic current densities were rarely reported before, they were detected occasionally as insolates data points and were often disregarded [26, 27]. Particularly, Li et al. [20] reported anodic current densities at an electrode being preferentially corroded under a simulated disbonded coating, but no explanation regarding how their segmented electrode was capable of detecting anodic currents under CP was presented.

A key concept needed to understand the probe's working principle is that the current registered by each electrode of the array is net current resulting from all anodic and cathodic processes occurring at its surface. Consequently, the factors affecting this process along the crevice and uncovered areas have a marked effect on the currents registered. It has been previously reported in the literature that parameters such as potential [8, 9, 11-22], pH [8-10, 12-17], oxygen concentration [9, 10, 12, 15-18] and concentration of other species [8-11] change considerably along disbonded areas. At the CP potential evaluated in this work (it is the minimum protection potential accepted by pipeline industry), dissolved oxygen concentration is the main factor affecting the cathodic reactions rate.

A schematic Evan's diagram showing the effect of oxygen depletion on the currents measured by the array is presented in Figure 3. The larger oxygen reduction limiting current case ($i_{Lim.1}$) represents the conditions at the uncovered electrodes, where the oxygen concentration is high. At this location, cathodic current densities ($i_{Lim.1}$) are larger than anodic current ($i_{corr.CP}$) and therefore, the net current densities measured by the array electrodes (I_{M1}) are cathodic despite some anodic reaction (i.e. corrosion reaction) may still take place ($i_{corr.CP}>0$). When considering the lower oxygen reduction limiting current case ($i_{Lim.2}$) that corresponds to the nearly depleted oxygen environment in the crevice area, the anodic current densities ($i_{corr.CP}$) could be larger than cathodic currents ($i_{Lim.2}$). Consequently, the current densities measured at this location are anodic (I_{M2}) even though both locations were considered at same CP potential in this hypothetical case. In real systems, the local CP potential within the crevice could be less negative than at its opening. In addition, pH and other solution compositional changes may also affect the anodic reaction rate. Nevertheless, none of these changes affect the rate of the diffusion controlled cathodic reaction, and consequently, in the absence of other cathodic reaction, the measurement of anodic current densities under the

Figure 3. Schematic Evan's diagram of the probe's working principle

simulated disbonded coating should remain valid. We believe this discussion explains the electrode array's capability to detect anodic currents under CP under disbonded coatings.
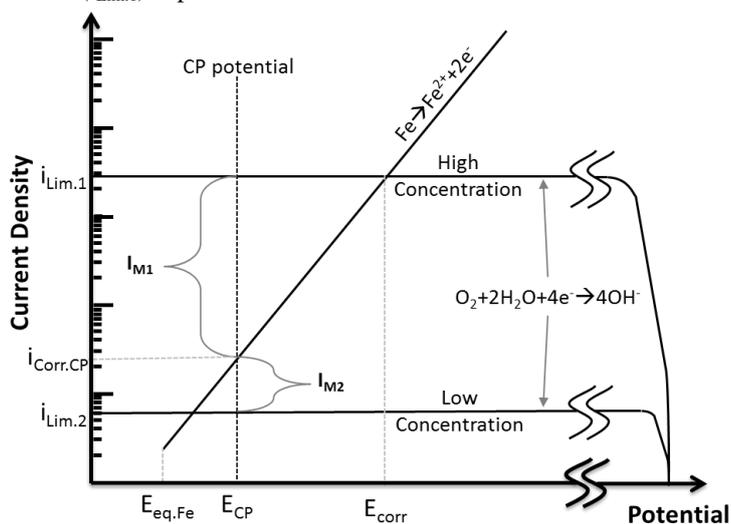
Figure 5 shows a comparison between the appearance of the electrode array surface at the end of the test period and the metal losses calculated form the probes data. A photograph of the electrode array is presented in Figure 5a where corrosion can be observed mainly on areas under the simulated disbonded coating. Figure 5b presents the metal losses calculated based on the anodic current densities detected by the probe using Faraday's law. The calculated metal losses, expressed as the thickness reduction after 23hs of exposure, shown values below 0.2µm indicating the high sensitivity of the probe. When comparing the measured (Fig. 5b) and actual (Fig. 5a) corrosion patterns, a good correlation in the general corrosion patterns for the electrodes located within the crevice is found. However, no metal loses were detected at the top three rows of electrodes. As was explained before, the high oxygen concentration at these locations prevents the probe from measuring anodic current densities at these locations. A more advanced data analysis technique capable of estimating corrosion from the cathodic current densities measured by the array at this location is being developed to overcome this limitation and will be published elsewhere.
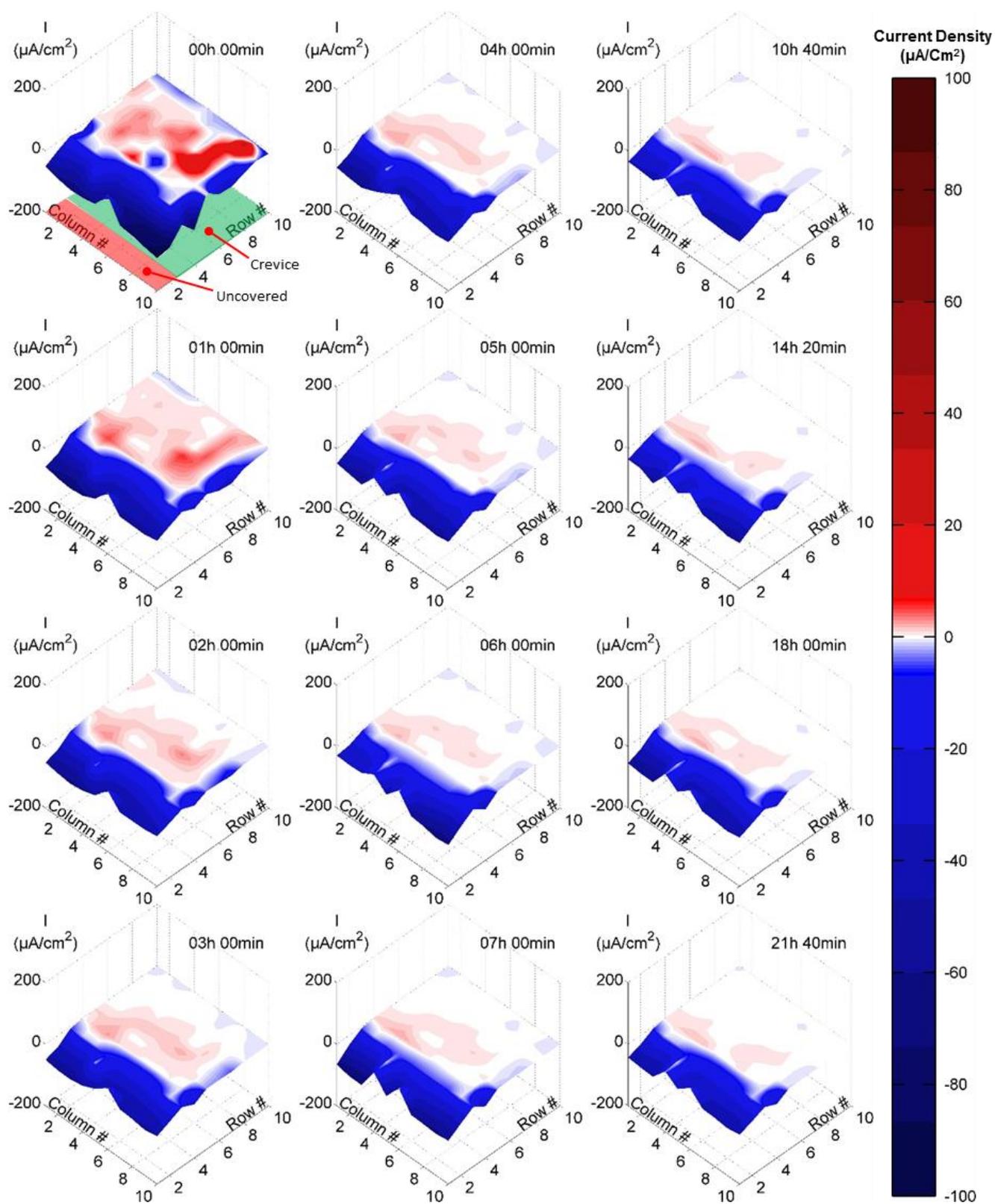
Figure 4. Current density distribution maps at several immersion times in 0.001M Na_2SO_4 at -760mV$_{Ag/AgCl}$.
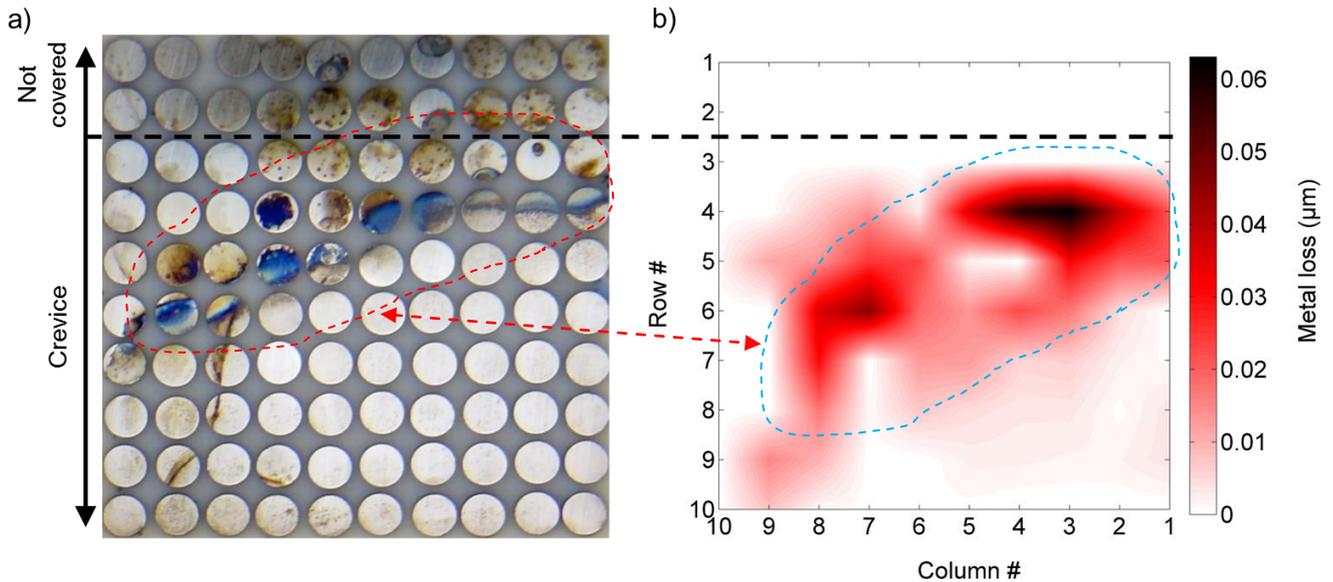
Figure 5. Comparison between actual (a) and measured (b) corrosion patterns.

CONCLUSIONS

A new probe has been designed to perform electrochemical measurements of corrosion rates, as well as CP effectiveness, under cathodically protected disbonded coatings in highly resistive media. The probe's capability to measure anodic current densities under CP, without requiring its interruption, was demonstrated in high resistivity aqueous solution. The pattern of calculated metal losses correlated well with the corrosion products distribution observed at the array surface.

ACKNOWLEDGMENTS

REFERENCES

[1]   Jankowski J, Electrochemical methods for corrosion rate determination under cathodic polarisation conditions - A review part I - DC methods, Corrosion Reviews 20(3) (2002) 159-177.

[2]   Jankowski J, Electrochemical methods for corrosion rate determination under cathodic polarisation conditions - A review part 2 - AC methods, Corrosion Reviews 20(3) (2002) 179-200.

[3]   Varela Facundo, Tan Yong Jun, Forsyth Maria, Hinton Bruce and Bonar Craig, A review of techniques for the monitoring of cathodic shielding and corrosion under disbonded coatings, (In) Proc. 53th Annual Conference of the Australasian Corrosion Association, 2013, Brisbane, Australia.

[4]   Shipilov SA and Le May I, Structural integrity of aging buried pipelines having cathodic protection, Engineering Failure Analysis 13(7) (2006) 1159-1176.

[5]   Abedi SS, Abdolmaleki A and Adibi N, Failure analysis of SCC and SRB induced cracking of a transmission oil products pipeline, Engineering Failure Analysis 14(1) (2007) 250-261.

[6]   Hasan F, Iqbal J and Ahmed F, Stress corrosion failure of high-pressure gas pipeline, Engineering Failure Analysis 14(5) (2007) 801-809.

[7]   Manfredi C and Otegui JL, Failures by SCC in buried pipelines, Engineering Failure Analysis 9(5) (2002) 495-509.

[8]   Yan M, Wang J, Han E and Ke W, Local environment under simulated disbonded coating on steel pipelines in soil solution, Corrosion Science 50(5) (2008) 1331-1339.

[9]   Song FM and Sridhar N, Modeling pipeline crevice corrosion under a disbonded coating with or without cathodic protection under transient and steady state conditions, Corrosion Science 50(1) (2008) 70-83.

[10]   Chin DT and Sabde GM, Modeling Transport Process and Current Distribution in a Cathodically Protected Crevice, Corrosion 56(8) (2000) 783-793.

[11]   Xu J, Sun C, Yan M and Wang F, Electrochemical behavior of steel A36 under disbonded coating in the presence of sulfate-reducing bacteria, Materials Chemistry and Physics 142(2–3) (2013) 692-700.

[12]   Chen X, Li XG, Du CW and Cheng YF, Effect of cathodic protection on corrosion of pipeline steel under disbonded coating, Corrosion Science 51(9) (2009) 2242-2245.
[13]   Eslami A, Fang B, Kania R, Worthingham B, Been J, Eadie R and Chen W, Stress corrosion cracking initiation under the disbonded coating of pipeline steel in near-neutral pH environment, Corrosion Science 52(11) (2010) 3750-3756.
[14]   Eslami A, Kania R, Worthingham B, Boven GV, Eadie R and Chen W, Effect of CO2 and R-ratio on near-neutral pH stress corrosion cracking initiation under a disbonded coating of pipeline steel, Corrosion Science 53(6) (2011) 2318-2327.
[15]   Perdomo JJ and Song I, Chemical and electrochemical conditions on steel under disbonded coatings: the effect of applied potential, solution resistivity, crevice thickness and holiday size, Corrosion Science 42(8) (2000) 1389-1415.
[16]   Perdomo JJ, Chabica ME and Song I, Chemical and electrochemical conditions on steel under disbonded coatings: the effect of previously corroded surfaces and wet and dry cycles, Corrosion Science 43(3) (2001) 515-532.
[17]   Song FM, Predicting the chemistry, corrosion potential and corrosion rate in a crevice formed between substrate steel and a disbonded permeable coating with a mouth, Corrosion Science 55(0) (2012) 107-115.
[18]   Chin DT and Sabde GM, Current Distribution and Electrochemical Environment in a Cathodically Protected Crevice, Corrosion 55(3) (1999) 229-237.
[19]   Song FM, Field Procedures to Estimate Corrosion Potentials and Rates and Cathodic Protection Penetration Limit in a Coating Disbonded Region on Buried Pipelines, Corrosion 66(3) (2010) 035005.
[20]   Li Z, Gan F and Mao X, A study on cathodic protection against crevice corrosion in dilute NaCl solutions, Corrosion Science 44(4) (2002) 689-701.
[21]   Eslami A, Kania R, Worthingham B, Boven GV, Eadie R and Chen W, Corrosion of X-65 Pipeline Steel Under a Simulated Cathodic Protection Shielding Coating Disbondment, Corrosion 69(11) (2013) 1103-1110.
[22]   Jack TR, Van Boven G, Wilmott M, Sutherby RL and Worthingham RG, Cathodic protection potential penetration under disbonded pipeline coating, Materials Performance 33(8) (1994) 17-21.
[23]   Tan YJ, The effects of inhomogeneity in organic coatings on electrochemical measurements using a wire beam electrode: Part I, Progress in Organic Coatings 19(1) (1991) 89-94.
[24]   Tan YJ and Yu ST, The effects of inhomogeneity in organic coatings on electrochemical measurements using a wire beam electrode: Part II, Progress in Organic Coatings 19(3) (1991) 257-263.
[25]   ASTM-D1193, Standard Specification for Reagent Water, ASTM International (Publishers), West Conshohocken, PA, 2011.
[26]   Brousseau R and Qian S, Distribution of Steady-State Cathodic Currents Underneath a Disbonded Coating, Corrosion 50(12) (1994) 907-911.
[27]   Wang W, Wang Q, Wang C and Yi J, Experimental studies of crevice corrosion for buried pipeline with disbonded coatings under cathodic protection, Journal of Loss Prevention in the Process Industries 29(0) (2014) 163-169.

AUTHOR DETAILS

F. N. Varela, is a PhD Student in the Institute for Frontier Materials at Deakin University, working on an Energy Pipeline CRC sponsored project. His PhD project is on corrosion monitoring technologies.

M. YJ. Tan is a Professor in Applied Electrochemistry and Corrosion Technologies at Deakin University in Australia, and is an Energy Pipeline Cooperative Research Centre Program Leader. His work spanned the range from academic teaching and research to industry consultancy and commercialisation. His main research outputs include methods for measuring and monitoring localised corrosion and other heterogeneous electrodes processes. He invited the wire beam electrode (WBE) method and contributed to the subsequent development of its theory and an industrial corrosion probe. He also contributed to the understanding of the electrochemical noise resistance and the modelling of complex electrochemical impedance spectroscope for practical engineering applications.

Professor M. Forsyth completed her PhD in January 1990 at Monash University and moved to Northwestern University to take up a Fulbright Fellowship in the area of solid electrolytes for lithium batteries. On her return to Melbourne she worked at DSTO for a year before joining the Department of Materials Engineering as a Lecturer in 1993. In 2001 she was awarded an ARC Professorial Fellowship and in 2011 became an Australian Laureate Fellow. She is currently the Chair in Electromaterials and Corrosion Sciences at Deakin University, within the Institute for Frontier Materials (IFM). She is also the Associate Director in the ARC Australian Centre of Excellence for Electromaterials Science.

Professor B. Hinton has an Honours degree in Metallurgy from the University of Queensland, Department of Mining and Metallurgical Engineering, and a PhD in Corrosion Engineering from University of Manchester (UMIST). During a long career at DSTO, he was involved with research in the areas of atmospheric corrosion, corrosion inhibition, metal finishing, stress corrosion cracking, corrosion sensors, and corrosion fatigue and hydrogen embrittlement. During that period he has also acted extensively as a consultant to RAAF, RAN and ARMY, in the field of corrosion prevention and control in aircraft structures. He is currently an Adjunct Professor at both Deakin and Monash Universities, where he provides advice and guidance to post graduate students.